Clays and Clay Minerals, Vol. 29, No. 6, 454–458, 1981.

NOTES

HYDROTHERMAL VERMICULITE FROM THE ATLANTIS II DEEP, RED SEA

Key Words—Atlantis II Deep, Hydrothermal, Iron, Red Sea, Vermiculite.

Major attention has in recent years been focused on the hot brines and their deposits in the Red Sea, chiefly because of their high content of heavy metals and their potential economic significance. The hot-brine environment has also yielded a series of clay-size, but morphologically well-developed aluminosilicates. Such euhedral particles of clay minerals have not yet been reported from any other marine hydrothermal deposits. Bischoff (1972) reported "ferroan nontronite" as a major component of the upper 5 m of the Atlantis II Deep deposits. Smectite, illite, palygorskite, chlorite, and sepiolite were reported by Roesch and Scheuermann (1974) in the upper parts of the hydrothermal deposits from both the Atlantis II and the Discovery Deeps, and a dioctahedral, iron-rich smectite was described by Goulart (1976) from the siliceous facies of the Atlantis II Deep.

In the course of a detailed mineralogical examination of the Chain 100-3-7 core taken by the R/V Chain in 1971, a sequence of authigenic clay minerals was observed that included vermiculite. To the author's knowledge this is the first reported occurrence of hydrothermal marine vermiculite. The present paper describes the mineralogical and chemical properties of this material and discusses its origin from volcanic ejecta.

MATERIALS AND METHODS

Core CHN 100-3-7 was taken from the SW-Basin of the Atlantis II Deep at 21°19.8′N and 38°05.2′E, from a water depth of 2048 m (Figure 1). The total core length was 1191 cm. Samples taken at various depths in the core were washed in distilled water and subjected to ultrasonic dispersion. They were then rewashed in 1 N NaCl and the excess salt removed. The Na-saturated and dispersed samples were then resus-

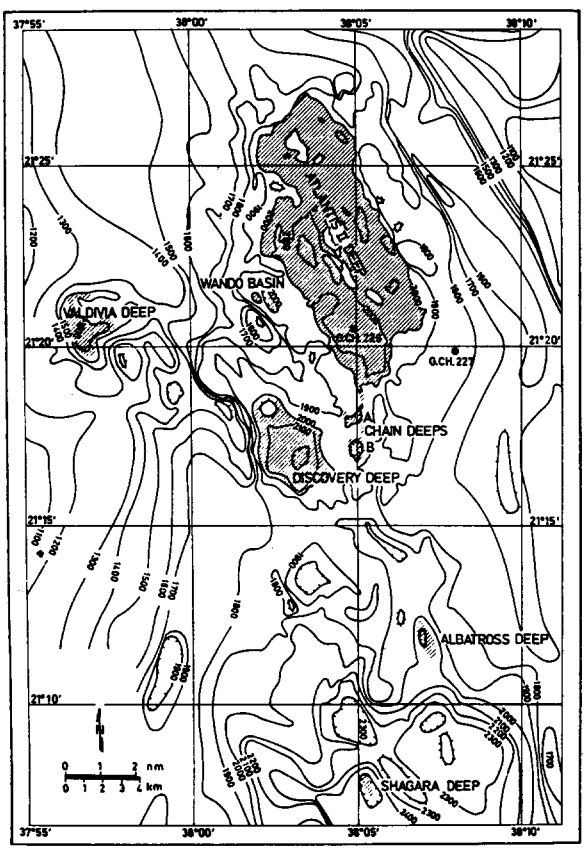

Figure 1. Location map of Atlantis II and neighboring Deeps in the Red Sea; the sites of the Glomar Challenger borings, drilled in 1972, are indicated; the site of the CHN 100-3-7 core is somewhat southeast of G.CH. 226 (after Bäcker and Richter, 1973).

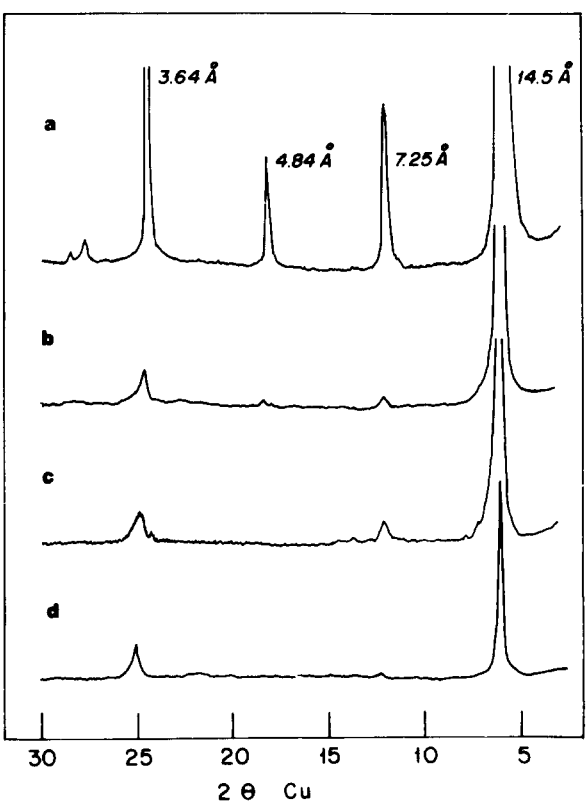

Figure 2. X-ray powder diffraction patterns of air-dried, oriented, Mg-saturated clay (<2 μm) from CHN 100-3-7 core samples from depths of (a) 1135 cm, (b) 990 cm, (c) 864 cm, (d) 880 cm; intensity scale: (a) 1000 c/sec; (b) 2000 c/sec; (c) and (d) 400 c/sec.

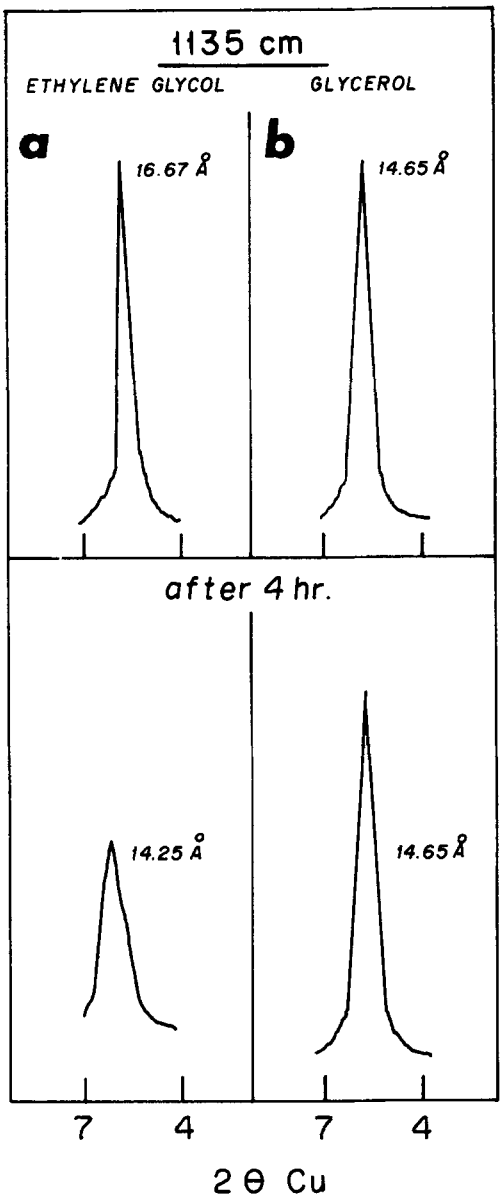

Figure 3. X-ray powder diffraction patterns of Mg-saturated, glycolated (a) and glycerolated (b) clay samples from a core depth of 1135 cm.

pended in distilled water, and the clay (<2 μm) fractions were separated by sedimentation and dried at 60°C.

X-ray powder diffraction (XRD) analyses were made with a Philips PW 1050/25 diffractometer equipped with a monochromator using CuKα radiation. Thermogravimetric analyses were performed on a combined DTA-TGA Mettler apparatus. Transmission electron microscopy was carried out on a Siemens (Elmiscope 100) instrument. Prior to diffractometry, free iron oxides were removed by the DCB method (Mehra and Jackson, 1960). Samples were saturated with ethylene glycol or glycerine prior to XRD examination via the vapor method. The chemical composition of Mg-saturated samples was determined after HF decomposition in Teflon-lined pressure vessels by atomic absorption spectrophotometry. The cation-exchange capacity (CEC) was determined by sodium saturation.

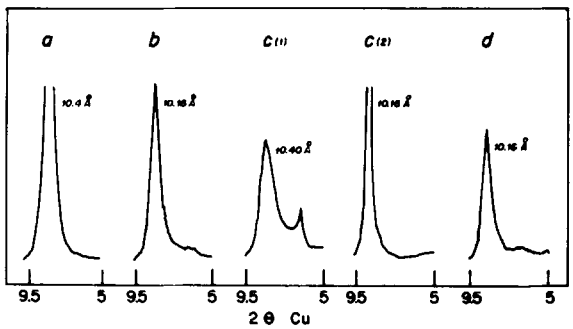

Figure 4. X-ray powder diffraction patterns of K-saturated clay from CHN 100-3-7 core samples, from depths of (a) 1135 cm, (b) 990 cm, (c-1) 864 cm, (c-2) 864 cm (after heating to 350°C), (d) 880 cm.

RESULTS

X-ray powder diffraction

Oriented mounts of a deferrated, Mg-saturated sample from a core depth of 1135 cm gave a series of integral basal spacings at 14.5, 7.25, 4.84, 3.64, and 2.88 Å, representing the 001, 002, 003, 004, and 005 reflections, respectively (Figure 2). The relative intensities of these reflections were in the order 002 < 004 < 001, characteristic of vermiculite. The 001 spacing of a Na-saturated sample was 12.45 Å. Immediately upon glycolation, the 001 spacing increased to 16.7 Å but shrank after a 4-hr exposure to air to 14.25 Å (Figure 3). The 001 spacing of the glycerol-saturated sample remained at 14.65 Å. Potassium saturation of the sample, followed by exposure to a relative humidity of 30–40%, caused the 001 reflection to collapse to 10.4 Å (Figure 4), and heating to 550°C for 2 hr collapsed the 001 spacing to 10.9 Å.

The method of distinguishing vermiculite from smectite is a subject of controversy. Neither the glycol- nor the glycerol-determined smectite-vermiculite boundary coincides with the definition proposed by the AIPEA Nomenclature Committee (Bailey, 1980) which chose an arbitrary charge of 0.6 equivalents per half unit cell to divide smectites from vermiculites. The ethylene glycol test tends to overestimate smectite and the glycerol test to underestimate it, as compared with the AIPEA definition (Środoń and Eberl, 1980). The contraction of the 001 spacing upon K-saturation and the formation of only one glycerol interlayer rather than two support the identification of the above mineral as a low-charge vermiculite.

Although the XRD patterns of air-dried, deferrated Mg-clays from other depths in this same core were similar (though of weaker intensity) to that from a depth of 1135 cm, the changes in basal spacings following the various treatments suggested an interlayering of the vermiculite with iron hydroxides. At a depth of 990 cm the collapse on K-saturation was incomplete, a distinct shoulder appearing towards smaller angles (Figure 4). This shoulder was even more prominent in samples from shallower parts of the core. Upon heating to 350°C the K-saturated clays collapsed uniformly to 10.2 Å. In a sample from a depth of 864 cm, K-saturation resulted in a doublet at 13.8 Å and 10.4 Å, suggesting the presence of two different phases. Heating the Mg-saturated samples to 550°C resulted in a collapse to 10.2–10.5 Å. Immediately following glycolation, doublets at 16.4 Å and 14.0 Å were noted for Mg-saturated samples from core depths of 880 and 864 cm, suggesting the presence of phases that accept temporarily 2 layers of organic molecules, together with other phases that accept

https://doi.org/10.1346/CCMN.1981.0290607 Published online by Cambridge University Press

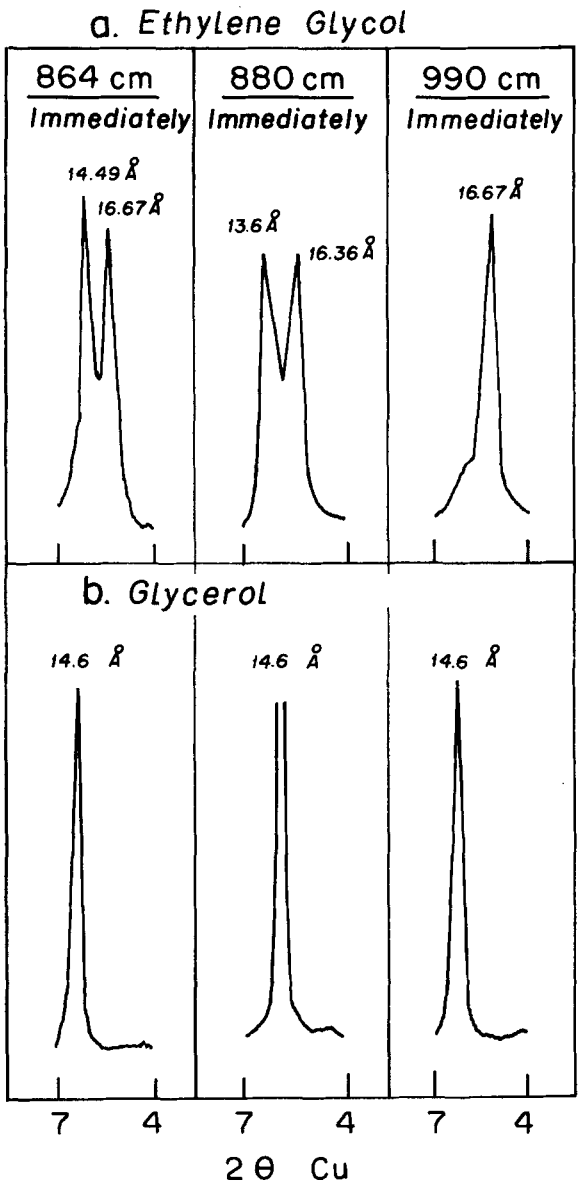

Figure 5. X-ray powder diffraction patterns of Mg-saturated, glycolated (a) and glycerolated (b) clay samples from core CHN 100-3-7.

only one layer (Figure 5). After 1–2 hours, the spacing of all glycolated samples returned to 14.6 Å. Glycerol expansion of the 001 spacings was not noted for any sample.

Thermal analysis

Differential thermal analysis (DTA) and differential thermal gravimetric (DTG) curves of the Na-saturated clay from a depth of 1135 cm are given in Figure 6. The curves are characterized by two major peaks: a very large endothermic peak associated with a major weight loss at 125°C, and a much weaker endothermic peak at 738°C, also associated with a weight loss. The curves resemble those reported by Mackenzie (1970) for saponite and vermiculite. The relatively low temperature at the peak associated with the expulsion of adsorbed water is due to the low hydration energy of adsorbed Na. The

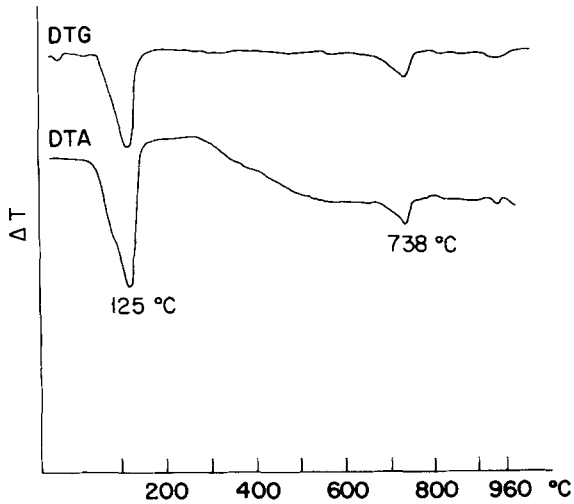

Figure 6. Differential thermal analysis (DTA) and differential thermal gravimetric (DTG) curves of Na-saturated clay from a core depth of 1135 cm in core CHN 100-3-7.

high temperature of the peak associated with the dehydroxylation process is characteristic of trioctahedral clay minerals. The exothermic effect that follows the dehydroxylation endotherm in DTA curves of some vermiculites was not observed. The broad, very shallow endothermic effect between 300° and 600°C probably represents the gradual release of strongly held interlayer water.

Transmission electron microscopy

Probably the most outstanding characteristic of the vermiculite from core CHN 100-3-7 is its well-defined morphology, as seen in Figures 7a–7d. Well-dispersed samples display rectilinear particles of a somewhat elongated habit, with dimensions of 1–2 μm by 0.5–1.0 μm. Hexagonal shapes are common, and the particles resemble those of the synthetic vermiculite reported by Douglas (1977). Some of the plates are rimmed with tiny, (0.05–0.2 μm), elongated, opaque particles, possibly iron oxides (Figure 7c).

Chemical composition

The chemical composition, CEC, and free iron oxides content of some of the vermiculitic layers are given in Table 1. Only two of the samples, layers from core depths of 1135 cm and 864 cm, exceed the threshold exchange capacities of 0.6 equivalents per half unit cell proposed by the AIPEA Nomenclature Committee (Bailey, 1980) to distinguish smectite from vermiculite. The clays from the other vermiculitic layers have exchange capacities that are significantly lower, suggesting interlayering or admixed mineral phases or both.

The clay from a depth of 1135 cm contains only 1.16% free iron oxides and from XRD examination appears to be composed almost exclusively of vermiculite. Structural (hydroxyl) water (4–5%), calculated from thermogravimetric curves, is lower than that reported for most vermiculites. The approximate structural formula of the deferrated, Mg-saturated clay, calculated from its chemical composition, is:

$$(Si_{6.83}Al_{1.17})(Al_{0.57}Fe^{3+}{}_{1.06}Fe^{2+}{}_{0.16}Mg_{3.30})O_{21.4}$$
$$(OH)_{2.6}(Mg_{0.51}Ca_{0.09}Na_{0.21}K_{0.04})$$

The formula suggests that nearly all of the charge deficiency arises in the tetrahedral layer due to extensive substitution of Si by Al. The cation occupancy in the octahedral layer is mid-

https://doi.org/10.1346/CCMN.1981.0290607 Published online by Cambridge University Press

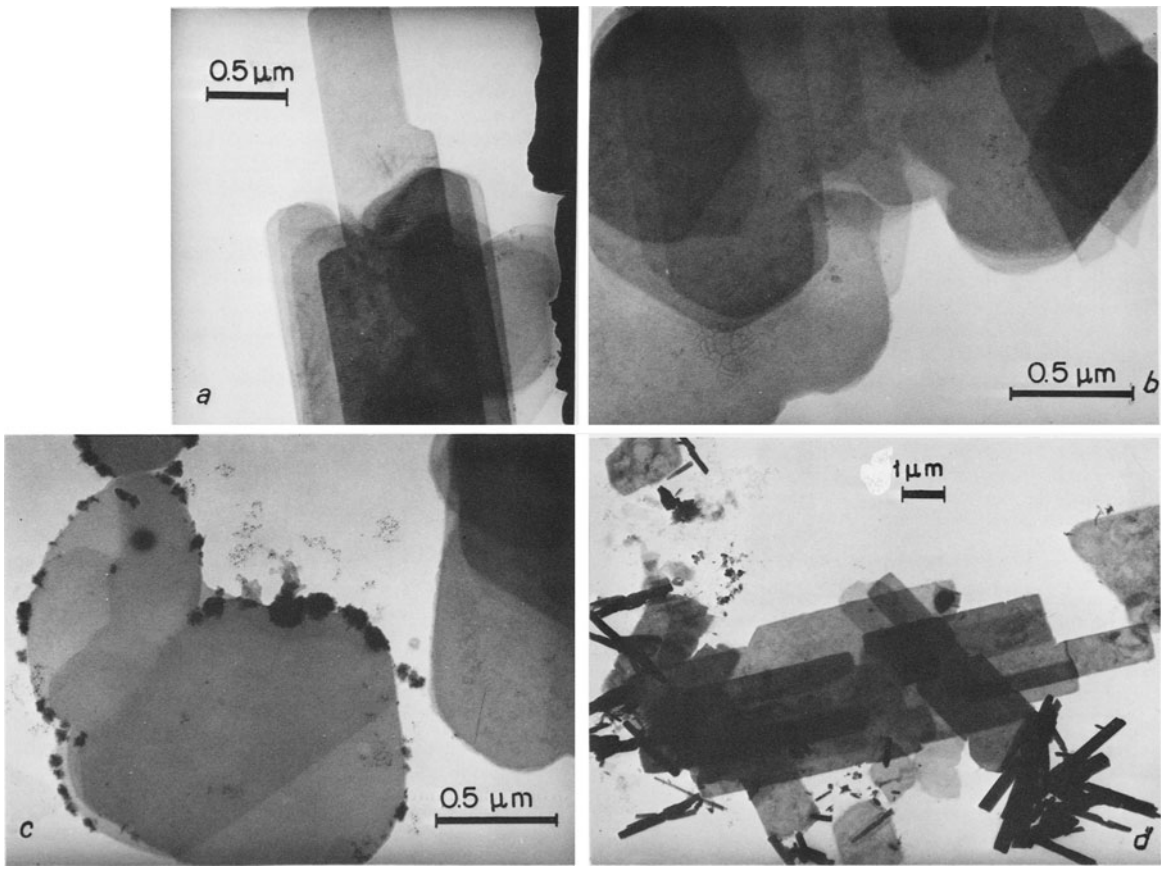

Figure 7. Transmission electron micrographs of Na-saturated clay (<2 μm) from CHN 100-3-7 core samples; a, b, and c from a depth of 1135 cm; d from a depth of 990 cm. Thin, tabular, elongated particles, commonly displaying a hexagonal habit, comprise the bulk of the material; Narrow, thick tabular laths of an unidentified phase are visible in the sample from a core depth of 990 cm. The tiny, elongated, opaque particles rimming the plates in Figure 7c are possibly ore minerals.

way between that of ideal dioctahedral and trioctahedral populations and resembles that reported by Barshad and Kishk (1969) for vermiculitic soil clays. Nearly all of the iron is Fe^{3+}, and some of the ferric iron may possibly be in tetrahedral sites, similar to the iron vermiculites described by Taylor *et al.* (1968). The small discrepancy between the determined CEC and the charge deficiency as calculated from the formula may be due to inaccuracies in the Fe^{2+} determination.

In samples from higher parts of the core, the Mg content is lower and the iron content is higher. The CEC is lower also, indicating interlayering and/or the presence of additional mineral phases, mainly opaque minerals.

DISCUSSION

The southwestern basin of the Atlantis II Deep is interesting in that it is the deepest and most active part of the Deep and also the influx site for most of the metallogenic solutions. The most recent volcanic ejecta have also been found here (Bäcker and Richter, 1973), and it is the only part of the Deep where talc has been reported in the silicate facies. Traces of talc in the Atlantis II Deep and the Port Sudan Deep were interpreted by Schneider and Schumann (1979) as a diagnostic feature of hydrothermally affected clays. Talc and serpentine were identified as major clay components in the bottom portions (at 1170 and 1183 cm) of the CHN core taken from the SW Basin (Al-

Table 1. Chemical composition of the clay fractions (<2 μm) from some vermiculitic clays in core CHN 100-3-7.

	Depth in core			
	1135 cm	900 cm	851 cm	864 cm
SiO_2	45.56	54.25	38.91	37.36
Al_2O_3	9.87	9.54	7.37	7.70
Fe_2O_3	10.59	15.67	24.25	31.30
FeO	1.28	—	2.56	n.d.
MgO	16.95	6.06	8.88	8.60
CaO	0.55	0.78	1.71	0.85
Na_2O	0.72	0.25	0.67	1.10
K_2O	0.17	0.17	0.35	0.19
MnO	0.10	0.16	0.23	0.17
ZnO	0.03	n.d.	0.64	0.11
CuO	0.03	n.d.	0.25	0.80
NiO	n.d.	n.d.	0.02	0.01
L.O.I.	15.40	12.98	15.20	13.00
Total	101.25	99.86	101.04	101.18
(free) Fe_2O_3[1]	1.16	8.15	6.15	14.95
CEC (meq/100 g)	137	59	119	128

[1] Dithionite extractable.

https://doi.org/10.1346/CCMN.1981.0290607 Published online by Cambridge University Press

Karghuli, 1979). Talc and serpentine are common products of hydrothermal processes (Moody, 1976). A hydrothermal origin of the Fe-vermiculite from a core depth of 1135 cm is also suggested by its euhedral outlines.

Although continental occurrences of hydrothermal vermiculite are numerous (Bassett, 1963), this is the first report of such material in a marine formation. The mineral described probably formed by precipitation from solutions supersaturated with respect to Si, Mg, and Fe in a manner similar to that proposed for Fe-smectite (Bischoff, 1972). The required Mg was most likely supplied by halmyrolytic decomposition products of the basic volcanic ejecta which abound in this region.

The relatively small amount of heavy metals in the vermiculitic clays of the CHN 100-7-3 core (Table 1) contrasts with the large amounts of Zn and Cu reported for nontronite (Bischoff, 1972; Goulart, 1976). However, when the nontronite from these nontronite-containing samples was carefully isolated, the heavy metal content of the smectite was found to be relatively low (Brockamp *et al.*, 1978). These data suggest that only a relatively small portion of the heavy metals present in the clay-brine slurries is in solid solution in the clay mineral structures.

ACKNOWLEDGMENTS

The senior author is indepted to the Minerva Foundation of the Max Planck Institute for granting a fellowship at Heidelberg University where this work was carried out. Special thanks are due to Dr. D. Ross from Woods Hole Oceanographic Institution for providing the core samples.

Department of Soil and Water Science ARIEH SINGER
The Hebrew University of Jerusalem
P.O. Box 12, Rehovet, 76-100, Israel

Institut für Sedimentforschung PETER STOFFERS
Universität Heidelberg
6900 Heidelberg 1, West Germany

REFERENCES

Al-Karghuli, A. (1979) Roentgenographische Untersuchungen an Sedimenten aus dem Atlantis II-Tief, Rotes Meer: M.Sc. Thesis, University of Heidelberg, 48 pp. (unpublished).

Bäcker, H. and Richter, H. (1973) Die rezente hydrothermal sedimentare Lagerstatte Atlantis II-Tief im Roten Meer: *Geol. Rundsch.* **62,** 697–741.

Bailey, S. W. (1980) Summary of recommendations of AI-PEA Nomenclature Committee: *Clay Miner.* **15,** 85–93.

Barshad, I. and Kishk, F. M. (1969) Chemical composition of soil vermiculite clays as related to their genesis: *Contr. Mineral. Petrol.* **24,** 136–155.

Bassett, W. A. (1963) The geology of vermiculite occurrences: *Clays & Clay Minerals* **10,** 61–69.

Bischoff, J. L. (1972) A ferroan nontronite from the Red Sea geothermal system: *Clays & Clay Minerals* **20,** 217–223.

Brockamp, O., Goulart, E., Harder, H., and Heydemann, A. (1978) Amorphous copper and zinc sulfides in the metalliferous sediments of the Red Sea: *Contr. Mineral. Petrol.* **68,** 85–88.

Douglas, L. A. (1977) Vermiculites: in *Minerals in Soil Environments,* J. B. Dixon and S. B. Weed, eds., Soil Science Society of America, Madison, Wisconsin, 259–292.

Goulart, E. P. (1976) Different smectite types in sediments of the Red Sea: *Geol. Jb.* **D17,** 135–149.

MacKenzie, R. C., ed. (1970) *Differential Thermal Analysis:* Academic Press, New York, 775 pp.

Mehra, O. P. and Jackson, M. L. (1960) Iron oxide removal from soils and clays by a dithionite-citrate system buffered with sodium bicarbonate: *Clays & Clay Minerals* **7,** 317–327.

Moody, J. B. (1976) Serpentinization: a review: *Lithos* **9,** 125–138.

Roesch, H. and Scheuermann, L. (1974) Mineralogische Untersuchungen an Sedimenten des Atlantis II Tiefs. Valdivia Va 01/03 Rotes Meer-Golf von Aden: *Wissenschaftliche Ergebnisse* 1. Bundesanstalt fur Bodenforschung, Hannover, 54–81.

Schneider, W. and Schumann, D. (1979) Tonminerale in Normalsedimenten, hydrothermal beinflussten Sedimenten und Erzschlammen der Roten Meeres: *Geol. Rundsch.* **68,** 631–648.

Środoń, J. and Eberl, D. D. (1980) The presentation of X-ray data for clay minerals: *Clay Miner.* **15,** 317–320.

Taylor, G. L., Ruotsala, A. P., and Keeling, R. O., Jr. (1968) Analysis of iron in layer silicates by Mössbauer spectroscopy: *Clays & Clay Minerals* **16,** 381–391.

(Received 10 September 1980; accepted 16 March 1981)